

Proton-proton fusion in effective field theory

Xinwei Kong

TRIUMF, 4004 Wesbrook Mall, Vancouver, British Columbia, Canada V6T 2A3

Finn Ravndal

Institute of Physics, University of Oslo, N-0316 Oslo, Norway

(Received 18 May 2000; published 30 August 2001)

The rate for the fusion process $p + p \rightarrow d + e^+ + \nu_e$ is calculated using nonrelativistic effective field theory. Including the four-nucleon derivative interaction, results are obtained in next-to-leading order in the momentum expansion. This reproduces the effects of the effective range parameter. Coulomb interactions between the incoming protons are included nonperturbatively in a systematic way. The resulting fusion rate is independent of specific models and wave functions for the interacting nucleons. At this order in the effective Lagrangian there is an unknown counterterm which limits the numerical accuracy. Assuming the counterterm to have a natural magnitude, the result is consistent with previous nuclear physics calculations.

DOI: 10.1103/PhysRevC.64.044002

PACS number(s): 25.10.+s, 11.10.-z, 25.40.Lw, 26.65.+t

I. INTRODUCTION

One of the most important problems in modern physics is the nature and properties of neutrinos. These were for a long time thought to be massless and stable, but experiments during the last decade have consistently shown this to be incompatible with the observed neutrino oscillations [1]. Historically and even today the fusion processes in the Sun are among the few available and abundant sources of low-energy neutrinos available for experimental investigations. In order to study oscillations in the detected fluxes, one needs to be sure of the production rates in the different nuclear reactions taking place in the Sun.

The basic process is proton-proton fusion $p + p \rightarrow d + e^+ + \nu_e$. It was explained more than 60 years ago by Bethe and Critchfield when nuclear physics was still at a very primitive stage [2]. When the field had matured, it was reconsidered in the light of more modern developments by Salpeter who included effective range corrections [3]. Applications to the specific conditions we have in the Sun were investigated by Bahcall and May [4]. This work was later extended by Kamionkowski and Bahcall who also included the effects of vacuum polarization in the Coulomb interaction between the incoming protons [5]. In spite of the enormous progress in nuclear physics during this time, the methods and approximations made in these different calculations were essentially the same with a resulting accuracy in the fusion rate of a few percent. Including strong corrections due to mesonic currents at smaller scales, the uncertainty in the rate can be reduced to much less than one percent [6]. This is very impressive for a strongly interacting process at low energies where ordinary perturbation theory cannot be used.

In the light of the importance this fundamental process plays in connection with the solar neutrino production and possible neutrino oscillations, it is natural to reconsider the process from the point of view of modern quantum field theory instead of the old potential models used previously. A first attempt in this direction was made by Ivanov *et al.* [7]. In their relativistic model they obtained a result which was significantly different from the standard result based upon

conventional nuclear physics models. Subsequently it was pointed out by Bahcall and Kamionowski that their effective nuclear interaction was not consistent with what is known about proton-proton scattering at low energies where Coulomb effects are important [8]. In a more recent contribution this defect of their calculation was removed and better agreement with standard results have been obtained [9].

The approach of Ivanov *et al.* is based upon relativistic field theory and should in principle yield reliable results. But it is well known that it is very difficult to use consistently a relativistic formulation for bound states such as the deuteron. In addition, the fusion process considered here takes place at low energies and should therefore instead be described within a nonrelativistic framework. Then all the large-momentum degrees of freedom are integrated out and one is left with an effective theory involving only the physically important field variables. The underlying, relativistic interactions are replaced by nonrenormalizable local interactions with coupling constants which must be determined from experiments at low energies. Along these lines the proton-proton fusion rate has been calculated by Park, Kubodera, Min, and Rho using chiral perturbation theory in the low-energy limit [10]. They obtain results in very good agreement with previous nuclear physics calculations. This is to be expected since they make use of phenomenological nucleon wave functions which fit low-energy scattering data very well. The drawback is that the results cannot be derived in an entirely analytical way.

A more fundamental approach to nucleon-nucleon interactions at low energies has been formulated in terms of an effective theory for nonrelativistic nucleons [11–14]. It involves a few basic coupling constants which have been determined from nucleon scattering data at low energies. With no more free parameters to fit it can then be used to make predictions for a large number of other experimentally accessible quantities [15]. The effects of pions can be included using the established counting rules and higher order corrections can be derived in a systematic way. When the energy is sufficiently low as for the fusion process considered here, the effects of pions can be integrated out and absorbed into the

coupling constants of the contact interactions. The resulting effective field theory which is sometimes called EFT(\not{n}) then involves only nucleon fields [16]. In proton-proton scattering at low energies the Coulomb repulsion has a dominant role and can naturally be incorporated into this theory [17]. As a direct result one can derive the difference between the strong scattering length which should be approximately the same as in proton-neutron scattering, and the observed one which is modified by Coulomb effects. The relation is very similar to the old result by Jackson and Blatt [18]. Corrections due to effective-range interactions can also be included but with more difficulty due to highly divergent integrals involving Coulomb wave functions [19].

With this understanding of low-energy proton-proton elastic scattering, one can calculate the leading order result for the fusion process $p + p \rightarrow d + e^+ + \nu_e$ taking place at essential zero initial kinetic energy [20]. With the use of a non-standard representation of the Coulomb propagator, the result is in full agreement with the corresponding leading order nuclear physics result and depends only on the physical proton-proton scattering length. To next order in the effective field theory expansion, one can derive higher order corrections [21] which also have the same structure as the corresponding effective-range corrections from more standard nuclear physics [3,4]. However, at this order there appears an unknown counterterm in the effective Lagrangian which will enter as a correspondingly unknown term in the result for the fusion rate. It can be determined from other related reactions. When this is done, we will also have a more accurate and predictive result for the fusion rate.

In the next section we present the theoretical framework which in the following will be used to calculate the proton-proton fusion rate in next-to-leading order in the momentum expansion of the effective theory. This is done both for the proton-neutron and proton-proton sectors. A short summary of the leading order calculation is given in Sec. III followed by a more detailed calculation of the next-to-leading order corrections. The derivation of the rate is completed by the inclusion of the effects of the counterterm. Assuming for it a natural magnitude, our final result is estimated to have an uncertainty of 6–8%. This is significantly more than in other approaches where it is around 1% [5]. The most accurate calculation has been made by Schiavilla *et al.* [6] who obtained a value in the range 7.05–7.06 for the squared overlap integral $\Lambda^2(E=0)$. This is achieved by including the effects of vacuum polarization and an axial two-body current operator whose size is determined from tritium beta decay. In the present effective theory a corresponding accuracy can only be hoped for when the counterterm is accurately determined in some other processes. Finally, in an appendix we present a new and simpler method to regularize divergent integrals involving derivatives of the Coulomb wave functions at the origin.

II. THEORETICAL FRAMEWORK

In the fusion reaction $p + p \rightarrow d + e^+ + \nu_e$ at low energies the incoming protons are in an antisymmetric spin singlet state. The deuteron d has spin $S=1$ and the process is thus a

Gamow-Teller transition mediated by the weak axial current operator \mathbf{A}_- which also lowers the isospin by a unit. For a given kinetic energy E and relative velocity v_{rel} of the protons in the initial state, the reaction cross section is then given by the standard formula

$$\sigma(E) = \frac{G_A^2 m_e^5}{2\pi^3 v_{\text{rel}}} f(E) |\langle d | \mathbf{A}_- | pp \rangle|^2, \quad (1)$$

where the squared matrix element must be spin averaged. Here G_A is the weak axial vector coupling constant, m_e is the electron mass and $f(E)$ is the Fermi function resulting from the integration over the available phase space of the leptons in the final state [24]. The available energy in the process for fusion at rest is set by the neutron-proton mass difference $\Delta M = M_n - M_p$ which is 1.294 MeV and the deuteron binding energy $B = 2.225$ MeV. This gives an energy release of 0.93 MeV carried away by the leptons. The temperature in the core of the Sun is approximately 15×10^6 K which corresponds to an average proton momentum around $p = 1.5$ MeV and a much smaller energy. We will therefore in the following assume that the initial proton energy E approaches zero. The kinetic energy of the lepton pair will be much smaller than the momentum $\gamma = \sqrt{BM}$ of the bound nucleons with reduced mass $M/2$ in the deuteron. With the above value for the binding energy it follows that $\gamma = 45.7$ MeV and thus to a very good approximation one can just ignore the momentum transfer between the leptons and the nucleons.

The difficult part of calculating the fusion cross section (1) lies in the hadronic matrix element $T_{fi}(p) = \langle d | \mathbf{A}_- | pp \rangle$ which is a function of the initial proton momentum $p = \sqrt{EM}$. Its magnitude can easily be estimated [24]. When the proton momentum goes to zero, the pp wave function $\psi_p(r)$ becomes constant over the range of the deuteron. It is simply given by the Sommerfeld factor $C_\eta = e^{-\pi\eta/2} |\Gamma(1+i\eta)|$ where $\eta = \alpha M/2p$ characterizes the strength of the Coulomb repulsion between the protons [25]. The probability to find the two protons at the same point is therefore

$$C_\eta^2 = \frac{2\pi\eta}{e^{2\pi\eta} - 1}. \quad (2)$$

At very low energies when η gets large, it becomes exponentially small and is the dominant effect in the fusion reaction. Similarly, in lowest order the deuteron wave function is simply

$$\psi_d(r) = \sqrt{\frac{\gamma}{2\pi}} \frac{e^{-\gamma r}}{r}. \quad (3)$$

A rough estimate for the nuclear matrix element is then

$$T_{fi}(p) = \int d^3r \psi_d(r) \psi_p(r) = C_\eta \sqrt{\frac{8\pi}{\gamma^3}}. \quad (4)$$

This result sets the scale for the fusion rate. It is therefore natural to define the reduced matrix element [3]

$$\Lambda(p) = \sqrt{\frac{\gamma^3}{8\pi C_\gamma^2}} |T_{fi}(p)| \quad (5)$$

which contains all the interesting and important physics. It is expected to have a value of the order of one and is now the conventional way of presenting theoretical results for the fusion rate. The goal of the present paper is to calculate this number in a more model-independent way by purely analytical methods without using any other phenomenological input than the scattering lengths and effective ranges appearing in nucleon-nucleon scattering.

A. KSW effective field theory

During the last couple of years much progress has been made in understanding the low-energy properties of few-nucleon systems from the nonrelativistic effective field theory proposed by Kaplan, Savage, and Wise [11]. At these length scales the proton and neutron are considered to be structureless point particles described by a nucleon isodoublet $N^T = (p, n)$ Schrödinger field. For energies well below the pion mass m_π , all interactions including those due to pion exchanges, will be local. In the effective Lagrangian they can be thus represented by terms involving only the nucleon field and derivatives thereof in such a way that all the symmetries obeyed by the strong interactions are preserved. At the lowest energies only S waves will contribute. Including no more than terms of dimension eight in the derivative expansion, there are only two possible interaction terms in the Lagrangian parametrized by the coupling constants C_0 and C_2 . It can be written as

$$\begin{aligned} \mathcal{L}_0 = & N^\dagger \left(i\partial_t + \frac{\nabla^2}{2M} \right) N - C_0 (N^T \mathbf{\Pi} N) (N^T \mathbf{\Pi} N)^\dagger \\ & + \frac{1}{2} C_2 \{ (N^T \vec{\nabla}^2 \mathbf{\Pi} N) (N^T \mathbf{\Pi} N)^\dagger + \text{H.c.} \}, \end{aligned} \quad (6)$$

where the operator $\vec{\nabla} = (\vec{\nabla} - \vec{\nabla})/2$. The projection operators Π_i enforce the correct spin and isospin quantum numbers in the channels under investigation. More specifically, for spin-singlet interactions $\Pi_i = \sigma_2 \tau_2 \tau_i / \sqrt{8}$ while for spin-triplet interactions $\Pi_i = \sigma_2 \sigma_i \tau_2 / \sqrt{8}$. This theory is now valid below an upper momentum Λ which will be the physical cutoff when the theory is regularized that way. Since the pion field is integrated out, all its effects are soaked up in the two coupling constants C_0 and C_2 . Then the value of the cutoff Λ will be set by the pion mass m_π . In this momentum range all the main properties of few-nucleon systems are now in principle given by the above Lagrangian. More accurate results will follow from higher order operators in this field-theoretic description [16].

The effective Lagrangian (6) is nonrenormalizable and divergent loop integrals must be regularized. For this purpose one can use the OS scheme of Mehen and Stewart [26] which is a generalization of the original proposal by Gegelia

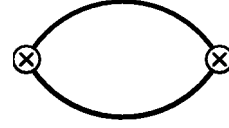


FIG. 1. Feynman diagram representing the leading order contribution to the deuteron wave function renormalization. The crosses represent the coupling to the interpolating field for the deuteron while the lines are nucleon propagators.

[13]. An equivalent method is the PDS scheme which was invented by Kaplan, Savage, and Wise [11,12] and is based on dimensional regularization. We will use it here. The *a priori* unknown coupling constants C_0 and C_2 can be determined in terms of experimental quantities measured in low-energy nuclear reactions. The size of the dimension-six coupling constant C_0 will then be determined by the scattering length a in nucleon-nucleon scattering while C_2 is found to be proportional to the effective range parameter r_0 . Both of these coupling constants will depend on the renormalization mass μ which enters in the PDS regularization scheme. It can be chosen freely in the interval $\gamma < \mu \leq m_\pi$ but physical results obtained from the effective theory should be independent of its precise value.

B. Proton-neutron interactions and the deuteron

The deuteron will appear as a bound state in proton-neutron scattering in the spin-triplet channel. It is then natural to determine the corresponding coupling constants by matching the results to properties at the deuteron pole of the scattering amplitude. The residue at the pole gives the renormalization constant Z of the deuteron interpolating field which replaces the wave function of the bound state [12]. In lowest order of perturbation theory one finds the renormalization constant from the irreducible two-point function $\Sigma(E)$ shown in Fig. 1. At the two vertices the interpolating field acts with energy E and zero momentum and a strength which we choose to be -1 . In the intermediate state there is a neutron and a proton which propagate with relative momentum \mathbf{k} . Integrating over all these momenta we then find the value of the diagram

$$\Sigma_0(E) = \int \frac{d^3k}{(2\pi)^3} \frac{1}{E - \mathbf{k}^2/M + i\epsilon}.$$

This divergent integral is now made finite using the PDS regularization scheme [11] and gives

$$\Sigma_0(E) = -\frac{M}{4\pi} (\mu - \sqrt{-ME}). \quad (7)$$

The renormalization constant

$$Z = \sqrt{\frac{1}{|d\Sigma/dE|_{E=-B}}} \quad (8)$$

which is evaluated at the deuteron pole where the binding energy is $B = \gamma^2/M$, thus takes the value $Z_0 = \sqrt{8\pi}\gamma/M$ at this order of perturbation theory. It is independent of the

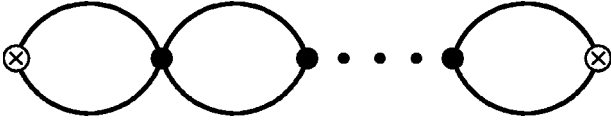


FIG. 2. Chain of proton-neutron interactions mediated by the leading order contact term.

coupling constant C_0^d whose effect must be summed to all orders in order to find the nonperturbatively bound state in this channel. When it takes the special renormalized value

$$C_0^d(\mu) = \frac{4\pi}{M} \frac{1}{\gamma - \mu} \quad (9)$$

we see that the reducible chain of bubble interactions in Fig. 2 just gives the same result as for the single bubble in the irreducible diagram in Fig. 1. In this particular channel one shall therefore not sum such chains of bubble diagrams when one describes the bound state deuteron by an interpolating quantum field. While the coupling constant C_0^d must be treated nonperturbatively, the effects of the derivative coupling C_2^d are included only to first order. The corresponding renormalized coupling constant is found to be $C_2^d(\mu) = \rho_d M [C_0^d(\mu)]^2 / 8\pi$ where $\rho_d = 1.76$ fm is the spin-triplet pn effective range scattering parameter evaluated at the deuteron pole [12,16]. It will also contribute to the renormalization constant Z via the perturbative diagram in Fig. 3 for the two-point function. It has the value $\Sigma_2(E) = C_2^d M E \Sigma_0^2(E)$ which gives the total contribution

$$Z_2 = Z_0 \left[1 - \frac{\gamma M}{2\pi} C_2^d(\mu - \gamma)(\mu - 2\gamma) \right]^{-1/2}. \quad (10)$$

In the limit $\mu \gg \gamma$ the dependence on the regularization mass μ is seen to go away. The previous value Z_0 then gets modified by the factor $\sqrt{Z_d} = 1/\sqrt{1 - \gamma\rho_d}$. This corresponds to a change of the normalization of the deuteron wave function (3) which now becomes $\psi_d(r) \rightarrow \sqrt{Z_d} \psi_d(r)$ in agreement with effective range theory in nuclear physics [27]. Here it is only valid at large distances since properties of the deuteron at scales less than $1/m_\pi$ are not accessible in this theory. Also, it is strictly only valid to first order in an expansion in powers of $\gamma\rho_d$ since it is obtained perturbatively in the coupling constant C_2^d . Since the expansion parameter has the rather large value $\gamma\rho_d = 0.41$, it is desirable to improve the convergence of perturbation theory in this coupling constant. This has recently been achieved by Phillips, Rupak, and Savage [23] whose method we will apply at the end of the more conventional approach we present first.

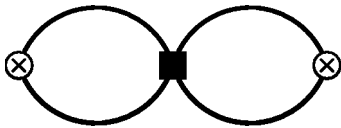


FIG. 3. Effective-range correction to the deuteron wave function renormalization constant.

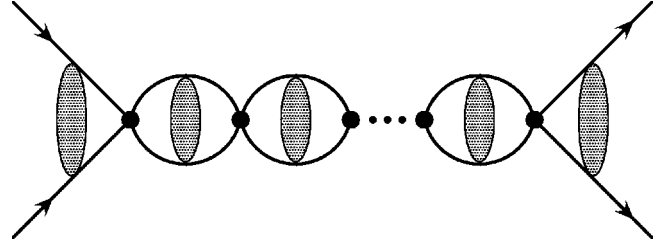


FIG. 4. Elastic scattering due to chain of bubble diagrams with Coulomb interactions. Incoming and outgoing particles are in Coulomb eigenstates.

C. Coulomb interactions and the proton-proton wave function

In the absence of strong interactions, the incoming proton-proton state with center-of-mass momentum \mathbf{p} is given by the Coulomb wave function [28]

$$\psi_{\mathbf{p}}(\mathbf{r}) = \frac{1}{\rho} \sum_{\ell=0}^{\infty} (2\ell+1) i^{\ell} e^{i\sigma_{\ell}} F_{\ell}(\rho) P_{\ell}[\cos(\theta)]. \quad (11)$$

Here $\rho = pr$ and $\sigma_{\ell} = \arg\Gamma(1 + \ell + i\eta)$ is the Coulomb phase-shift. At low energies only the S wave will contribute. It is given in terms of the Kummer function $M(a, b; z)$ as

$$F_0(\rho) = C_{\eta} \rho e^{-i\rho} M(1 - i\eta, 2; 2i\rho) \quad (12)$$

which is a confluent hypergeometric function.

The strong interactions between the protons can now be included using the same KSW Lagrangian (6) but now with coupling constants C_0^p and C_2^p which also get renormalized [19]. As in the proton-neutron channel one must again consider the coupling C_0^p to all orders in perturbation theory. In this way one finds that proton-proton elastic scattering is given by the infinite sum of all chains of Coulomb-dressed bubble diagrams as shown in Fig. 4. Each bubble is given by the Coulomb propagator

$$G_C(E; \mathbf{r}', \mathbf{r}) = M \int \frac{d^3q}{(2\pi)^3} \frac{\psi_{\mathbf{q}}(\mathbf{r}') \psi_{\mathbf{q}}^*(\mathbf{r})}{p^2 - q^2 + i\epsilon}. \quad (13)$$

It satisfies the Lippmann-Schwinger equation $G_C = G_0 + G_0 V_C G_C$ where V_C is the Coulomb potential and

$$G_0(E; \mathbf{q}', \mathbf{q}) = \frac{M}{p^2 - q^2 + i\epsilon} (2\pi)^3 \delta(\mathbf{q}' - \mathbf{q}) \quad (14)$$

is the free propagator in momentum space. Iterating this functional equation we see from Fig. 5 that it corresponds to the exchange of zero, one, two, and more static photons. Since a single bubble in Fig. 4 corresponds to the propaga-

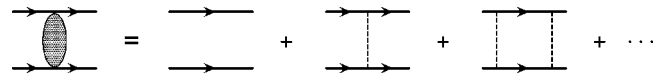


FIG. 5. The Coulomb propagator can be represented by an infinite sum of exchanged static photons between the two charged particles.

tion of the proton pair with energy $E=p^2/M$ from zero separation and back to zero separation, it has the value $J_0(p) = G_C(E; \mathbf{r}'=0, \mathbf{r}=0)$ or

$$J_0(p) = M \int \frac{d^3 q}{(2\pi)^3} \frac{2\pi\eta(q)}{e^{2\pi\eta(q)} - 1} \frac{1}{p^2 - q^2 + i\epsilon}. \quad (15)$$

The integral is seen to be ultraviolet divergent, but can be regularized in the PDS scheme in $d=3-\epsilon$ dimensions. When contributions from poles in $d=2$ dimensions are subtracted, one finds [17]

$$J_0(p) = \frac{\alpha M^2}{4\pi} \left[\frac{1}{\epsilon} + \ln \frac{\mu\sqrt{\pi}}{\alpha M} + 1 - \frac{3}{2} C_E - H(\eta) \right] - \frac{\mu M}{4\pi}. \quad (16)$$

Here $C_E=0.5772$ is Euler's constant and the function

$$H(\eta) = \psi(i\eta) + \frac{1}{2i\eta} - \ln(i\eta) \quad (17)$$

is known to appear in these Coulomb scattering problems [18]. The divergent $1/\epsilon$ piece will be absorbed in counterterms representing electromagnetic interactions at shorter scales. This replaces the bare coupling constant C_0^p with the renormalized value $C_0^p(\mu)$. It can be found by matching the calculated proton-proton scattering amplitude to the experimental one. This is usually given by the measured scattering length $a_p = -7.82$ fm when the proton momentum $p \rightarrow 0$. Thus one finds [17]

$$\frac{1}{C_0^p(\mu)} = \frac{M}{4\pi a_p} + J_0(0). \quad (18)$$

Since the function (17) is dominated by its real part $h(\eta) = 1/(12\eta^2) + \mathcal{O}(\eta^{-4})$ which goes to zero when $p \rightarrow 0$, we see from the form of $J_0(0)$ in Eq. (16) that it is natural to introduce the μ -dependent scattering length

$$\frac{1}{a(\mu)} = \frac{1}{a_p} + \alpha M \left[\ln \frac{\mu\sqrt{\pi}}{\alpha M} + 1 - \frac{3}{2} C_E \right], \quad (19)$$

where α is the fine-structure constant. It corresponds to the Jackson-Blatt relation between the strong and Coulomb-modified proton-proton scattering lengths [18]. Then we can write

$$C_0^p(\mu) = \frac{4\pi}{M} \frac{1}{1/a(\mu) - \mu} \quad (20)$$

which is now on the same form as Eq. (9) for the bound-state case.

In next order of the momentum expansion the derivative coupling C_2^p in Eq. (6) is introduced perturbatively. Again matching to low-energy proton-proton scattering, one finds $C_2^p(\mu) = \rho_d M [C_0^p(\mu)]^2 / 8\pi$ where $\rho_d = 2.79$ fm is the proton-proton effective range parameter. It is not affected by Coulomb corrections to this order in the effective theory. However, the C_2^p coupling gives an important contribution to

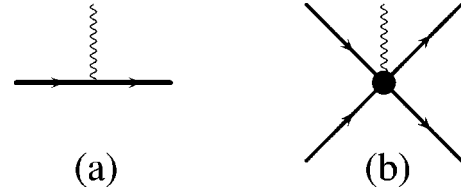


FIG. 6. One-body interaction in (a) represents the weak axial current vertex while the two-body interaction in (b) represents the higher order axial vector counterterm.

the scattering length (19) which picks up an additional term $-\mu\rho_d/2$ in the parentheses [19].

D. Gamow-Teller transition operators

The dominant weak transition matrix elements in the basic fusion rate formula (1) are due to the elementary isovector axial current operator

$$\mathbf{A}_-^{(1)} = N^\dagger \boldsymbol{\sigma} \tau_- N \quad (21)$$

which converts an incoming proton into a neutron with the proper spin and isospin quantum numbers. This is the ordinary one-body interaction depicted in Fig. 6(a). But when we include the dimension-eight derivative operator in Eq. (6) higher dimension weak transition operators must also be considered. These were first discussed by Butler and Chen in connection with elastic and inelastic scattering of neutrinos on deuterons [22]. In our case there is only one such operator which can be written as

$$\mathbf{A}_-^{(2)} = L_{1A} (N^T \mathbf{\Pi} N)^\dagger (N^T \mathbf{\Pi}_- N), \quad (22)$$

where the projection operator $\mathbf{\Pi} = \sigma_2 \boldsymbol{\sigma} \tau_2 / \sqrt{8}$ acts in the spin-triplet final proton-neutron state while $\mathbf{\Pi}_- = \sigma_2 \tau_2 \tau_- / \sqrt{8}$ acts on the spin-singlet proton-proton initial state. The weak axial vector coupling constant has been factored out so that the effective coupling constant is just L_{1A} . This new two-body operator represents weak transitions taking place at shorter length scales than considered in the effective theory and the corresponding vertex is shown in Fig. 6(b). Typically it represents transitions due to pion interactions and other two-body interactions. In the effective theory it will act as a counterterm which can absorb the dependence on the renormalization mass μ . Its actual magnitude is presently unknown. It can be estimated from dimensional arguments combined with the renormalization group. Even better would be to determine it in some other weak process where its contribution could be isolated and measured.

III. HADRONIC MATRIX ELEMENTS

We are now in position to calculate the hadronic matrix elements $T_{fi}(p) = \langle d | \mathbf{A}_- | pp \rangle$ of the weak transition operator. The initial proton state is constructed in terms of the Coulomb wave functions as in the elastic scattering case. For the final state deuteron we use the interpolating field which contains a proton-neutron state with the amplitude Z which is the wave function renormalization constant. We will initially

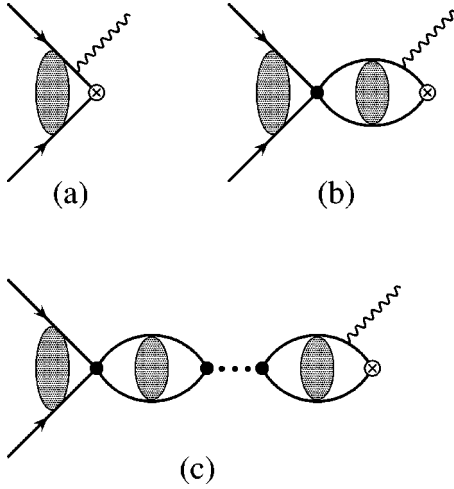


FIG. 7. Feynman diagrams contributing to proton-proton fusion in leading order.

consider only the action of the axial current operator (21). The effects of spin has been separated out and will not enter the following calculation.

A. Leading order result

In lowest order of the effective theory only the dimension-six operators will contribute with coupling constants C_0^d and C_0^p in the deuteron and proton-proton sectors, respectively. The transition matrix element T_{fi} then gets contributions from three classes of diagrams shown in Fig. 7. After being hit by the weak current, the proton-proton system is transformed into a bound deuteron. The value of the simplest diagram in Fig. 7(a) is then seen to be $Z_0 A_0(p)$ where Z_0 is the constant derived in the previous section and

$$A_0(p) = \int \frac{d^3k}{(2\pi)^3} \frac{M}{\mathbf{k}^2 + \gamma^2} \psi_{\mathbf{p}}(\mathbf{k}). \quad (23)$$

There is a factor (-1) from the deuteron vertex and the bound proton-neutron propagator is $-M/(\mathbf{k}^2 + \gamma^2)$. In addition, we have introduced the Fourier transform $\psi_{\mathbf{p}}(\mathbf{k})$ of the Coulomb wave function (11) when the protons have the center-of-mass momentum \mathbf{p} . Including next the strong interaction once between the two protons as shown in Fig. 7(b), we get the contribution $Z_0 C_0 B_0(p) \psi_{\mathbf{p}}(0)$, where

$$B_0(p) = \int \frac{d^3k}{(2\pi)^3} \frac{d^3k'}{(2\pi)^3} \frac{M}{\mathbf{k}^2 + \gamma^2} G_C(E; \mathbf{k}, \mathbf{k}') \quad (24)$$

is a convergent integral and the last factor $\psi_{\mathbf{p}}(0) = C_{\eta} e^{i\sigma_0}$ gives the amplitude for the two incoming protons to meet at the first vertex. Going to higher orders in the coupling C_0^p we will add in Coulomb-dressed bubble diagrams as in Fig. 7(c). Each bubble is of the same form as in proton-proton scattering in Fig. 4 where the contribution from each bubble is given by $J_0(p)$ in Eq. (15). Adding up these diagrams, they are seen to form a geometric series with the sum $C_0^p/(1$

$-C_0^p J_0$). The total contribution from all the three classes of diagrams thus gives the lowest order transition amplitude $T_{fi}(p) = Z_0 T_0(p)$, where

$$T_0(p) = \left[A_0(p) + B_0(p) \frac{C_0^p \psi_{\mathbf{p}}(0)}{1 - C_0^p J_0(p)} \right]. \quad (25)$$

The term involving C_0^p can now be expressed in terms of the proton-proton scattering length a_p in Eq. (18) and is independent of the renormalization scale μ .

For the explicit evaluation of this matrix element it is necessary to introduce the Coulomb wave function (12). Since the first term of the momentum integral is the product of two Fourier transformed functions, we find that it simplifies in coordinate space to

$$\begin{aligned} A_0(p) &= M C_{\eta} e^{i\sigma_0} \int_0^{\infty} dr r e^{-(\gamma+ip)r} M(1-i\eta, 2; 2ipr) \\ &= \frac{M C_{\eta} e^{i\sigma_0}}{(\gamma+ip)^2} {}_2F_1\left(1-i\eta, 2; 2; \frac{2ip}{\gamma+ip}\right). \end{aligned} \quad (26)$$

Now the hypergeometric function ${}_2F_1(a, b, b; z) = (1-z)^{-a}$ so that the final result can be written as

$$A_0(p) = C_{\eta} e^{i\sigma_0} \frac{M}{p^2 + \gamma^2} e^{2\eta \arctan(p/\gamma)}. \quad (27)$$

In the expression (24) for $B_0(p)$ we notice that the integral over \mathbf{k}' gives the complex conjugate value of the Coulomb wave function at the origin. It therefore takes the form

$$B_0(p) = M \int \frac{d^3k}{(2\pi)^3} \int \frac{d^3q}{(2\pi)^3} \frac{M}{\mathbf{k}^2 + \gamma^2} \frac{\psi_{\mathbf{q}}(\mathbf{k})}{\mathbf{p}^2 - \mathbf{q}^2 + i\epsilon} \psi_{\mathbf{q}}^*(0).$$

The integral over \mathbf{k} is just the previous result for $A_0(q)$ so that

$$B_0(p) = M \int \frac{d^3q}{(2\pi)^3} \frac{M}{q^2 + \gamma^2} \frac{e^{2\eta \arctan(q/\gamma)}}{p^2 - q^2 + i\epsilon} \frac{2\pi\eta(q)}{e^{2\pi\eta(q)} - 1}. \quad (28)$$

When the momentum of the incoming proton is nonzero it yields, in general, a complex result.

In the fusion limit $p \rightarrow 0$ we now find that the first term (27) simplifies to

$$A_0(p \rightarrow 0) = C_{\eta} \frac{M}{\gamma^2} e^{\chi + i\sigma_0}, \quad (29)$$

where the parameter $\chi = \alpha M/\gamma$. Similarly, the second term $B_0(p)$ becomes proportional to the integral

$$I(\chi) = \int_0^{\infty} dx \frac{2x}{e^x - 1} \frac{e^{(x/\pi)\arctan(\pi\chi/x)}}{x^2 + \pi^2\chi^2} \quad (30)$$

in the same limit when we use $x = 2\pi\eta(q)$ as a new integration variable. Repeating this calculation with a different rep-

resentation of the Coulomb Green's function, it can be shown that the integral takes the value [20]

$$I(\chi) = \frac{1}{\chi} - e^\chi E_1(\chi) \quad (31)$$

when expressed in terms of the exponential integral

$$E_1(\chi) = \int_\chi^\infty dt \frac{e^{-t}}{t}.$$

With $Z_0 = \sqrt{8\pi}\gamma/M$ for the renormalization constant, we thus find for the full matrix element the result

$$T_{fi} = \sqrt{\frac{8\pi}{\gamma^3}} C_\eta e^{i\sigma_0} [e^\chi - \alpha M a_p I(\chi)]. \quad (32)$$

The reduced matrix element in leading order is therefore

$$\Lambda_0(0) = e^\chi - \alpha M a_p I(\chi). \quad (33)$$

This is also the canonical result from standard nuclear physics [4]. The parameter $\chi = 0.15$ and thus the integral $I(0.15) = 4.96$. Combined with the measured value $a_p = -7.82$ fm for the scattering length, we then have $\Lambda_0(0) = 2.51$ for the reduced matrix element. In the formula for the fusion rate it gives the contribution $\Lambda_0^2(0) = 6.30$. From previous applications of the effective theory [15], we know that leading-order results are typically within 20–30% of the correct values. Going to next order in perturbation theory, the accuracy is expected to increase to 5–10%.

B. Effective range corrections

In next order of the momentum expansion of the effective field theory, there is no operator which induces S - D mixing of the deuteron state. It will first appear at one order higher [12]. The dimension-eight couplings C_2^d and C_2^p give the additional diagrams shown in Fig. 8 in first order perturbation theory. Each such operator V_2 has a momentum matrix element $\langle \mathbf{k} | V_2 | \mathbf{q} \rangle = C_2(\mathbf{k}^2 + \mathbf{q}^2)/2$. The contribution from Fig. 8(a) is seen to be

$$T_a = \frac{1}{2} C_2^d \int \frac{d^3k}{(2\pi)^3} \int \frac{d^3q}{(2\pi)^3} \frac{-M}{\mathbf{k}^2 + \gamma^2} (\mathbf{q}^2 + \mathbf{k}^2) \frac{M}{\mathbf{q}^2 + \gamma^2} \psi_{\mathbf{p}}(\mathbf{q}). \quad (34)$$

This can be expressed in terms of the divergent integral

$$I_0(\gamma) = -M \int \frac{d^3k}{(2\pi)^3} \frac{1}{\mathbf{k}^2 + \gamma^2} = \frac{-M}{4\pi} (\mu - \gamma) \quad (35)$$

which is the same as occurred in the lowest-order determination of the wave function renormalization constant in Eq. (7). It is finite after PDS regularization which gives for the other occurring integral

$$I_2(\gamma) = -M \int \frac{d^3k}{(2\pi)^3} \frac{\mathbf{k}^2}{\mathbf{k}^2 + \gamma^2} = -\gamma^2 I_0(\gamma) \quad (36)$$

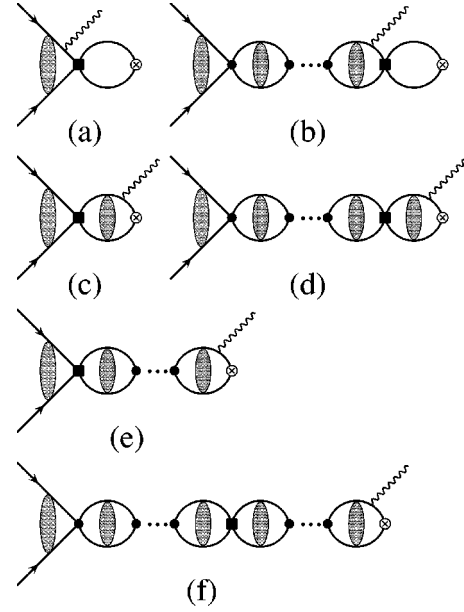


FIG. 8. Corrections to the fusion amplitude coming in at next-to-leading order.

since $\int d^d k / (2\pi)^d = 0$ in dimensional regularization. Together with the function $A_0(p)$ in Eq. (23) and the related function

$$A_2(p) = M \int \frac{d^3k}{(2\pi)^3} \frac{\mathbf{k}^2}{\mathbf{k}^2 + \gamma^2} \psi_{\mathbf{p}}(\mathbf{k}) \quad (37)$$

we thus have for the matrix element (34)

$$T_a = \frac{1}{2} C_2^d [I_2(\gamma) A_0(p) + I_0(\gamma) A_2(p)].$$

In the same way as we could express the integral $I_2(\gamma)$ in terms of $I_0(\gamma)$, we also find

$$A_2(p) = M \psi_{\mathbf{p}}(0) - \gamma^2 A_0(p). \quad (38)$$

Here $\psi_{\mathbf{p}}(0) = C_\eta e^{i\sigma_0}$ where σ_0 is the Coulomb S -wave phase shift. When we eventually use this result to calculate the fusion rate from Eq. (5), we will take the absolute value and this phase factor will not contribute. We therefore write

$$T_a = \frac{1}{2} C_2^d I_0(\gamma) [M C_\eta(p) - 2\gamma^2 A_0(p)],$$

where the same phase factor also should be dropped in the last term. This result is now to be taken in the fusion limit $p \rightarrow 0$ as in the previous section.

The contribution from Fig. 8(b) involves the Coulomb Green's function and its derivative in the triple integral

$$T_{b1} = \frac{1}{2} C_2^d C_0^p \int \frac{d^3 k}{(2\pi)^3} \int \frac{d^3 q}{(2\pi)^3} \int \frac{d^3 q'}{(2\pi)^3} G_C(E; \mathbf{q}, \mathbf{q}') \\ \times \frac{M}{\mathbf{q}^2 + \gamma^2} (\mathbf{q}^2 + \mathbf{k}^2) \frac{-M}{\mathbf{k}^2 + \gamma^2} \psi_{\mathbf{p}}(0)$$

resulting from just one proton bubble. This can be expressed in terms of the function $B_0(p)$ in Eq. (24) and the related function

$$B_2(p) = M \int \frac{d^3 k}{(2\pi)^3} \frac{d^3 q}{(2\pi)^3} \frac{\mathbf{k}^2}{\mathbf{k}^2 + \gamma^2} G_C(E; \mathbf{k}, \mathbf{q}) \quad (39)$$

as

$$T_{b1} = \frac{1}{2} C_2^d C_0^p [I_2(\gamma) B_0(p) + I_0(\gamma) B_2(p)] \psi_{\mathbf{p}}(0).$$

With the simplification

$$B_2(p) = M J_0(p) - \gamma^2 B_0(p) \quad (40)$$

we find the total contribution

$$T_b = \frac{1}{2} C_2^d \frac{I_0(\gamma) C_0^p}{1 - C_0^p J_0(p)} [M J_0(p) - 2\gamma^2 B_0(p)] C_\eta \quad (41)$$

from all the Coulomb-dressed proton bubble diagrams in Fig. 8(b). Here we have again replaced $\psi_{\mathbf{p}}(0)$ by $C_\eta(p)$.

The remaining diagrams involve the proton derivative coupling C_2^p . Figure 8(c) gives

$$T_c = \frac{1}{2} C_2^p \int \frac{d^3 q}{(2\pi)^3} \int \frac{d^3 k}{(2\pi)^3} \int \frac{d^3 k'}{(2\pi)^3} \frac{M}{\mathbf{k}'^2 + \gamma^2} G_C(E; \mathbf{k}', \mathbf{k}) \\ \times (\mathbf{k}^2 + \mathbf{q}^2) \psi_{\mathbf{p}}(\mathbf{q}). \quad (42)$$

This can again be expressed in terms of the functions $B_0(p)$ and $C_\eta(p)$ and their derivatives. In particular, we define

$$B'_2(p) = M \int \frac{d^3 k}{(2\pi)^3} \frac{d^3 q}{(2\pi)^3} \frac{\mathbf{q}^2}{\mathbf{k}^2 + \gamma^2} G_C(E; \mathbf{k}, \mathbf{q}) \quad (43)$$

and introduce

$$\psi_2(p) = \int \frac{d^3 k}{(2\pi)^3} \mathbf{k}^2 \psi_{\mathbf{p}}(\mathbf{k}) \quad (44)$$

which is the double derivative of the Coulomb wave function at the origin. Both of them are highly divergent, but can be calculated in the PDS regularization scheme and expressed in terms of already introduced functions. This is shown in the Appendix. We thus find for this diagram

$$T_c = \frac{1}{2} C_2^p [\psi_0(p) B'_2(p) + \psi_2(p) B_0(p)],$$

where $\psi_2(p) = -\alpha M \mu \psi_0(p)$ in the limit $p \rightarrow 0$ as shown in the Appendix. Then we also have $B'_2(p) = M I_0(\gamma) - \alpha M \mu B_0(p)$ and we therefore get

$$T_c = \frac{1}{2} C_2^p C_\eta [M I_0(\gamma) - 2\alpha M \mu B_0(p)] \quad (45)$$

which now involves only finite and known quantities.

In Fig. 8(d) we sum over all the Coulomb-dressed proton bubbles. The result is given by the multiple integral

$$T_d = \frac{1}{2} C_2^p \frac{C_0^p}{1 - C_0^p J_0(p)} \int \frac{d^3 k}{(2\pi)^3} \int \frac{d^3 k'}{(2\pi)^3} \int \frac{d^3 q}{(2\pi)^3} \int \frac{d^3 q'}{(2\pi)^3} \\ \times G_C(E; \mathbf{q}, \mathbf{q}') (\mathbf{q}^2 + \mathbf{k}^2) G_C(E; \mathbf{k}', \mathbf{k}) \frac{M}{\mathbf{k}'^2 + \gamma^2} \psi_{\mathbf{p}}(0).$$

Again we can reorder the integrand so that the result is expressed in terms of simpler functions

$$T_d = \frac{1}{2} C_2^p \frac{C_\eta C_0^p}{1 - C_0^p J_0(p)} [J_2(p) B_0(p) + J_0(p) B'_2(p)],$$

where now

$$J_2(p) = \int \frac{d^3 k}{(2\pi)^3} \int \frac{d^3 q}{(2\pi)^3} \mathbf{k}^2 G_C(E; \mathbf{k}, \mathbf{q}) \quad (46)$$

involves the derivative of the Coulomb propagator. It is also evaluated in the Appendix. In the limit $p \rightarrow 0$ we find $J_2(p) = -\alpha M \mu J_0(p)$ which together with the related result for $B'_2(p)$ gives

$$T_d = \frac{1}{2} C_2^p \frac{C_\eta C_0^p J_0(p)}{1 - C_0^p J_0(p)} [M I_0(\gamma) - 2\alpha M \mu B_0(p)]. \quad (47)$$

It has the same structure as T_c in Eq. (45) and they can therefore be combined into a simpler result.

The deuteron side of the diagrams in Fig. 8(e) is seen to be just $B_0(p)$. Summing up the bubbles on the proton side, we find

$$T_e = \frac{1}{2} \frac{C_2^p C_0^p}{1 - C_0^p J_0(p)} [J_2(p) \psi_0(p) + J_0(p) \psi_2(p)] B_0(p).$$

In the limit $p \rightarrow 0$ this simplifies again with the result

$$T_e = -C_2^p C_\eta \frac{C_0^p J_0(p)}{1 - C_0^p J_0(p)} \alpha M \mu B_0(p). \quad (48)$$

Similarly we find that the diagrams in Fig. 8(f) gives

$$T_f = \frac{1}{2} C_2^p \left(\frac{C_0^p}{1 - C_0^p J_0(p)} \right)^2 [J_2(p) J_0(p) \\ + J_0(p) J_2(p)] \psi_0(p) B_0(p)$$

which becomes

$$T_f = -C_2^p C_\eta \left(\frac{C_0^p J_0(p)}{1 - C_0^p J_0(p)} \right)^2 \alpha M \mu B_0(p) \quad (49)$$

in the low-energy limit $p \rightarrow 0$.

Adding now up the contributions from all the diagrams in Fig. 8, we obtain the sum

$$T_2 = -\gamma^2 C_2^d I_0(\gamma) T_0(p) + \frac{1}{2} (C_2^p + C_2^d) \frac{M I_0(\gamma) C_\eta}{1 - C_0^p J_0(p)} - \frac{\alpha M \mu C_2^p C_\eta B_0(p)}{[1 - C_0^p J_0(p)]^2},$$

where $T_0(p)$ is the lowest order matrix element (25). The full transition matrix element to this order is therefore

$$T_{fi} = Z_2 T_0(p) + Z_0 T_2(p),$$

where Z_2 is the next-to-leading order renormalization constant (10). Reordering and combining terms, we obtain

$$Z_0^{-1} T_{fi} = A_0(p) + B_0(p) C_\eta \left[\frac{C_0^p}{1 - C_0^p J_0(p)} - \frac{\alpha M \mu C_2^p}{[1 - C_0^p J_0(p)]^2} \right] + \frac{\gamma M}{4\pi} C_2^d(\mu) (\mu - \gamma)^2 \quad (50)$$

$$\times \left[A_0(p) + B_0(p) \frac{C_\eta C_0^p}{1 - C_0^p J_0(p)} \right] \quad (51)$$

$$- \frac{M^2}{8\pi} C_\eta (\mu - \gamma) \frac{C_2^p + C_2^d}{1 - C_0^p J_0(p)}. \quad (52)$$

In the bubble integral $J_0(p)$ we can take $p \rightarrow 0$ since it is finite. The function $B_0(p)$ is also finite in this limit while $A_0(p)$ becomes proportional to the Coulomb factor $C_\eta(p)$ which diverges. As shown previously in the application of the same effective theory to low-energy, elastic proton-proton scattering, the first square bracket is now just the physical proton-proton scattering length a_p calculated in next-to-leading order with the result [19]

$$a_p = \frac{M}{4\pi} \left(\frac{C_0^p}{1 - C_0^p J_0(0)} - \frac{\alpha M \mu C_2^p}{[1 - C_0^p J_0(0)]^2} \right). \quad (53)$$

The last term is the effective-range correction which is important in order to have a physically meaningful result for the scattering length. We see that when this is zero, we have the previous result (18) used in leading order.

The transition matrix element in next-to-leading order is now given by Eq. (52). Isolating a common factor, the reduced matrix element (5) follows as

$$\Lambda_2(0) = \Lambda_0(0) \left[1 + \frac{\gamma M}{4\pi} C_2^d(\mu) (\mu - \gamma)^2 \right] - a_p \gamma^2 (\mu - \gamma) \frac{C_2^p(\mu) + C_2^d(\mu)}{2C_0^p(\mu)}, \quad (54)$$

where $\Lambda_0(0)$ is the leading-order result (33) but now expressed in terms of the next-to-leading order scattering length (53). With the already established value for the coupling constant C_2^d we see that it is now multiplied by the factor $1 + \gamma \rho_d/2$. This can be interpreted as the first term in the expansion of the deuteron normalization factor Z_d discussed in the previous section. While this term in the result is independent of the renormalization scale μ , we see that the last term is generally not. However, when μ is much larger than the other mass scales given by the scattering lengths, this dependence goes away and we are left with the definite result

$$\Lambda_2(0)_{\mu \gg \gamma} = \Lambda_0(0) [1 + \frac{1}{2} \gamma \rho_d] + \frac{1}{4} a_p \gamma^2 (\rho_p + \rho_d). \quad (55)$$

It has a structure which is very similar to the reduced matrix element in the standard nuclear physics effective-range approximation [3,4]

$$\Lambda_{\text{ER}}(0) = \sqrt{Z_d} [\Lambda_0(0) + \frac{1}{4} a_p \gamma^2 (\rho_p + \rho_d)]. \quad (56)$$

With the known values for the different nucleon parameters, the result in this old approximation is therefore $\Lambda_{\text{ER}}(0) = 2.66$ or $\Lambda_{\text{ER}}^2(0) = 7.08$. On the other hand, our next-to-leading order result (55) gives $\Lambda_2(0)_{\mu \gg \gamma} = 2.54$ which is just a 1.4% addition to the leading order result we previously obtained. This is surprisingly small, but results from an almost total cancellation between the two effective-range corrections in Eq. (55). The net result for the squared matrix element is $\Lambda_2^2(0)_{\mu \gg \gamma} = 6.45$ which is seen to be 8% below the effective-range value.

C. Contribution from counterterm

A complete calculation of the fusion rate in next-to-leading order must include all operators contributing to this order in the momentum expansion of effective theory. Until now we have only included the effects of the dimension-8 operators coupling four nucleons with a derivative interaction. Since our result above in general depends on the renormalization scale, it signals that the calculation is incomplete. There should be additional interaction terms that in principle should absorb all dependence on the renormalization scale. This is in fact the case as shown by Butler and Chen [22] and discussed in the introductory section. It has the structure as given in Eq. (22) and corresponds to the weak current coupling directly to the four-nucleon vertex. In a more fundamental theory it could be due to weak interactions via virtual pions, coupling to excited nucleons or more general two-body operators in nuclear physics language. Obviously, this counterterm will also modify the numerical result for the fusion rate in addition to softening the μ dependence.

In our case it gives a contribution depicted by the Feynman diagram in Fig. 9(a). It is similar to the previously calculated contribution from Fig. 8(a) in Eq. (34) and becomes

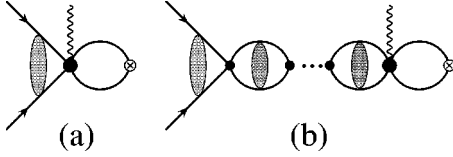


FIG. 9. Contributions to the fusion amplitude from the counterterm.

$$T_a^{ct} = L_{1A} \int \frac{d^3k}{(2\pi)^3} \int \frac{d^3q}{(2\pi)^3} \frac{M}{\mathbf{k}^2 + \gamma^2} \psi_{\mathbf{p}}(\mathbf{q}) = -L_{1A} C_{\eta} J_0(\gamma). \quad (57)$$

The strong interactions in the initial state, now to lowest order in the derivative expansion, gives the series of diagrams shown in Fig. 9(b). They form again an infinite geometric series whose sum

$$T_b^{ct} = -L_{1A} C_{\eta} J_0(\gamma) \frac{C_0^p J_0(p)}{1 - C_0^p J_0(p)} \quad (58)$$

is given by the proton-proton physical scattering length a_p from Eq. (18) and $a(\mu)$ from Eq. (20) in the fusion limit $p \rightarrow 0$. With the regularized value for the integral I_0 , we thus find the total contribution from the counterterms to be

$$T^{ct} = -L_{1A} C_{\eta} \frac{M}{4\pi} (\mu - \gamma) \left[\mu - \frac{1}{a(\mu)} \right] a_p. \quad (59)$$

The corresponding reduced matrix element then follows from Eq. (5) after multiplication by the wavefunction renormalization constant Z_0 .

We now include this new contribution as a correction to the matrix element (54) coming from the ordinary axial current interactions. For the combined result we then have

$$\Lambda_2^{ct}(0) = \Lambda_0(0) \left[1 + \frac{1}{2} \gamma \rho_d \right] - \frac{a_p \gamma^2}{4\pi} (\mu - \gamma) \left[\mu - \frac{1}{a(\mu)} \right] \times \left[L_{1A}(\mu) - \frac{M}{2} [C_2^p(\mu) + C_2^d(\mu)] \right]. \quad (60)$$

The coupling constant L_{1A} of the counterterm must have a dependence on the renormalization scale μ so that the total μ dependence in the last term is negligible. When $\mu \gg \gamma$ we see that this requirement leads to

$$L_{1A}(\mu)_{\mu \gg \gamma} = \frac{4\pi \ell_{1A}}{M \mu^2}, \quad (61)$$

where ℓ_{1A} is an unknown dimensionless constant. It is set by physics on scales shorter than $1/m_{\pi}$ and its natural value should be around one as pointed out in Ref. [22] In order to get a rough idea of the sensitivity of the result on this parameter, we take $\mu = m_{\pi}$ which is the scale at which one should match the effective theory to the more fundamental theory involving pions. Then varying ℓ_{1A} in the interval $[-1, 1]$, we find that the fusion rate measured by $|\Lambda_2^{ct}(0)|^2$ varies linearly from 6.22 to 6.84. These values are seen to be

systematically below the effective-range result following from Eq. (56), but are within the 5–10 % uncertainty range expected at this order.

D. Z_d parametrization

It has already been pointed out that our results for the proton-proton fusion have a very similar structure to what one finds in the effective-range approximation in nuclear physics. This has also been seen in other processes investigated within the same effective theory and at higher orders in the perturbative expansion [12,16]. It is understood when one realizes that these processes are dominated by the properties of the deuteron wave function at large distance scales which is contained in the effective-range approximation. In the KSW field theory, these properties are coded into the coupling constants C_0^d and C_2^d . While C_0^d is responsible for binding the deuteron and must be treated nonperturbatively, the effects of C_2^d are to be treated perturbatively and gives the detailed behavior of the wave function at large distances. In the above C_2^d was determined by matching to the effective range parameter ρ_d . In order to get better agreement with low-energy proton-neutron scattering data which are related directly to the deuteron bound state wave function via analytical continuation, it has been pointed out by Phillips, Rupak and Savage that one should instead match C_2^d to the wave function normalization parameter Z_d [23]. This gives the result

$$C_2^d(\mu) = \frac{2\pi}{\gamma M} \frac{Z_d - 1}{(\mu - \gamma)^2}, \quad (62)$$

where $Z_d = 1.69$. They have shown that this markedly improves the convergence of the perturbative calculation of many processes involving deuterons at low energies. Rupak has recently applied this improved method to neutron-proton fusion $n + p \rightarrow d + \gamma$ at energies relevant to big-bang nucleosynthesis as discussed above [30]. Including one higher order in the perturbative expansion of the electric transition amplitude, he has then obtained an accuracy of 1% for the calculated cross section.

In our case we can now use this new value for C_2^d in the result (54) for the reduced matrix element. Including also the counterterm as in Eq. (60), we then obtain our final result. Again the counterterm coupling constant will have the form (61) for large values of the renormalization mass. Choosing $\mu = m_{\pi}$, we now find that $\Lambda_2^2(0)$ varies between 7.04 and 7.70 when the parameter ℓ_{1A} takes values in the interval $[-1, 1]$. With the size of the unknown counterterm in this range, we thus have the central value $\Lambda_2^2(0) = 7.37$ with a conservative estimate for the uncertainty of 6–8%. We thus find a somewhat higher value for the fusion rate in this improved perturbative calculation compared with results from effective range theory (56) and the inclusion of axial two-body effects [6]. It is to be expected that when this calculation is extended to higher orders, these different ways of determining the coupling constant C_2^d will not matter so much for the final result. As a representative value for the fusion rate from effective field theory at this stage, we can

take the average of our two central values with and without Z_d parametrization and thus obtain a result in better agreement with the standard nuclear physics result.

IV. DISCUSSION AND CONCLUSION

Effective field theory is a very powerful approach to low-energy physics. It can hardly be said to be wrong when used correctly since it is just based upon the basic symmetries of the problem and standard quantum field theory. In that way it is a very conservative approach since it does not admit assumptions about the physics on scales shorter than it is meant to handle. Instead of such specific and model-dependent assumptions, one has higher-dimensional contact interactions and counterterms with coupling constants which represent the unknown physics. The most common criticism against effective field theory is therefore that it is not accurate enough since the results may depend on one or more such coupling constants which are not *a priori* known. One can make estimates of these unknown coupling constants based upon some kind of naturalness supported by dimensional analysis and the renormalization group.

But these counterterms do not really represent a weakness of effective field theory. Since they are interactions appearing in a Lagrangian, they will appear with the same strength in many different processes. If one or more of these allow for the determination of the corresponding coupling constants, one can then make much more accurate predictions for the other reactions. One recent example is radiative neutron-proton capture $n + p \rightarrow d + \gamma$. When the process takes place at very low energies or at rest, it is dominated by a magnetic dipole transition which at next-to-leading order also involves a four-nucleon counterterm very similar to the one we have considered here for proton-proton fusion. From the measured rate at these low energies, the counterterm can then be determined numerically [16]. The same neutron-proton fusion process is also a key reaction in big-bang nucleosynthesis where it takes place at energies upto around 1 MeV. Chen and Savage have now calculated the corresponding cross section with an uncertainty of 4% based on the measured counterterm [29]. A similar accuracy can be expected also for proton-proton fusion if the counterterm can be determined.

In principle the counterterm could be measured in many other reactions, but most of them are either insensitive to the counterterm or involve three body interactions. For example in inelastic scattering of neutrinos on deuterons at SNO, this unknown term will enter both the charged-current and neutral-current cross sections linearly and approximately with the same size as shown by Butler, Chen, and Kong [22]. But since only the ratio between these two processes will be measured accurately, the counterterm cannot be determined with the required precision in these experiments. However, similar reactions initiated by antineutrinos from reactors where the fluxes are known, could be useful. The unknown counterterm could also be determined in tritium β decay when we know how to describe it by effective field theory. Some progress has already been made in this direction [31]. As shown by Rupak for radiative neutron capture, with an accurately measured counterterm, we should then be in the

position to obtain the proton-proton fusion rate with much less uncertainty. This will place our understanding of this fundamental process on a more solid basis. Needless to say, it will also strengthen our knowledge of the neutrino production rate in the Sun.

Note added. During the editorial process a new paper by Butler and Chen [32] appeared where the fusion rate is calculated within the same effective theory including interactions to two orders higher in the derivative expansion. These new results reduce significantly the uncertainties in the present paper, but the problem with the unknown counterterm persists.

ACKNOWLEDGMENTS

We want to thank John Bahcall, Jiunn-Wei Chen, Peter Lepage, Gautam Rupak, Martin Savage, and Mark Wise for encouragement and many helpful discussions. Most of this work was done in the Department of Physics and INT at the University of Washington in Seattle and we are grateful for generous support and hospitality.

APPENDIX

We will here regularize and evaluate the divergent integrals involving Coulomb wave functions which are needed for the effective-range corrections to the fusion rate. Some of them have previously been encountered in connection with higher order corrections to low-energy proton-proton elastic scattering [19]. They were then calculated by a method based on regularization of the Fourier-transformed Coulomb wavefunctions. We will here use a different and simpler method.

The simplest integral is $J_2(p)$ in Eq. (46) which we rewrite as

$$J_2(p) = p^2 J_0(p) + \int \frac{d^3 k}{(2\pi)^3} \int \frac{d^3 q}{(2\pi)^3} (\mathbf{k}^2 - \mathbf{p}^2) \langle \mathbf{k} | G_C(E) | \mathbf{q} \rangle.$$

It represents a Coulomb-dressed bubble propagator with a derivative interaction at one vertex. Here we have introduced the free eigenmomentum states $\langle \mathbf{k} |$ and $| \mathbf{q} \rangle$. The Coulomb propagator $G_C(E)$ satisfies the Lippmann-Schwinger equation $G_C = G_0 + G_0 V_C G_C$ where $G_0(E)$ is the free propagator (14) and V_C is the Coulomb potential. In momentum space it has the matrix element $\langle \mathbf{k} | V_C | \mathbf{k}' \rangle = 4\pi\alpha / (\mathbf{k} - \mathbf{k}')^2$. The first term will now give zero with the use of dimensional regularization

$$\int \frac{d^d k}{(2\pi)^d} = 0. \quad (\text{A1})$$

We then insert two complete sets of momentum eigenstates between the three operators in the matrix elements in the second term. The denominator in the free propagator G_0 then cancels against the factor $\mathbf{k}^2 - \mathbf{p}^2$ in the integral. We are thus left with

$$\begin{aligned} & \int \frac{d^3k}{(2\pi)^3} (\mathbf{k}^2 - \mathbf{p}^2) \langle \mathbf{k} | G_0 V_C G_C | \mathbf{q} \rangle \\ &= -M \int \frac{d^3k}{(2\pi)^3} \int \frac{d^3k'}{(2\pi)^3} \frac{4\pi\alpha}{(\mathbf{k} - \mathbf{k}')^2} \langle \mathbf{k}' | G_C(E) | \mathbf{q} \rangle. \end{aligned}$$

In the integral over \mathbf{k} we now shift the integration variable $\mathbf{k} \rightarrow \mathbf{k} + \mathbf{k}'$ and use the PDS regularization result

$$\int \frac{d^3k}{(2\pi)^3} \frac{4\pi\alpha}{\mathbf{k}^2} = \alpha\mu. \quad (\text{A2})$$

The remaining two integrals over \mathbf{k}' and \mathbf{q} then simply gives $J_0(p)$. We thus have the result

$$J_2(p) = [p^2 - \alpha M \mu] J_0(p). \quad (\text{A3})$$

Except for a higher order term in the fine-structure constant α , this agrees with what we obtained with the much more cumbersome wavefunction regularization method [19].

The next integral $\psi_2(p)$ in Eq. (44) corresponds to the double derivative of the Coulomb wave function at the origin. We can write it as

$$\psi_2(p) = p^2 \psi_0(p) + \int \frac{d^3k}{(2\pi)^3} (\mathbf{k}^2 - \mathbf{p}^2) \langle \mathbf{k} | \psi_{\mathbf{p}} \rangle,$$

where $|\psi_{\mathbf{p}}\rangle$ is a Coulomb state with momentum \mathbf{p} . It can formally be expressed in terms of the free state $|\mathbf{p}\rangle$ as

$$|\psi_{\mathbf{p}}\rangle = [1 + G_C V_C] |\mathbf{p}\rangle.$$

One then has

$$\begin{aligned} & \int \frac{d^3k}{(2\pi)^3} (\mathbf{k}^2 - \mathbf{p}^2) \langle \mathbf{k} | \psi_{\mathbf{p}} \rangle \\ &= \int \frac{d^3k}{(2\pi)^3} (\mathbf{k}^2 - \mathbf{p}^2) [\langle \mathbf{k} | G_0 V_C | \mathbf{p} \rangle + \langle \mathbf{k} | G_0 V_C G_C V_C | \mathbf{p} \rangle] \\ &= \int \frac{d^3k}{(2\pi)^3} (\mathbf{k}^2 - \mathbf{p}^2) \langle \mathbf{k} | G_0 V_C | \psi_{\mathbf{p}} \rangle \end{aligned}$$

using $G_C V_C | \mathbf{p} \rangle = |\psi_{\mathbf{p}}\rangle - |\mathbf{p}\rangle$ in the last term. Inserting now again two complete sets of free momentum states as above, it follows that

$$\psi_2(p) = p^2 \psi_0(p) - M \int \frac{d^3k}{(2\pi)^3} \int \frac{d^3q}{(2\pi)^3} \frac{4\pi\alpha}{(\mathbf{k} - \mathbf{q})^2} \langle \mathbf{q} | \psi_{\mathbf{p}} \rangle.$$

After a shift of integration variable, we have the result

$$\psi_2(p) = [p^2 - \alpha M \mu] \psi_0(p) \quad (\text{A4})$$

when making use the the PDS regularized integral (A2).

The last integral we need is $B'_2(p)$ in Eq. (43). Rewriting it as above, it takes the form

$$B'_2(p) = p^2 B_0(p) + M \int \frac{d^3k}{(2\pi)^3} \frac{d^3q}{(2\pi)^3} \frac{\mathbf{q}^2 - \mathbf{p}^2}{\mathbf{k}^2 + \gamma^2} G_C(E; \mathbf{k}, \mathbf{q}),$$

where the first term is the finite integral (24). In the second term we can use the Lippmann-Schwinger equation for the Coulomb propagator. Again we find that the denominator of the free propagator cancels against $\mathbf{q}^2 - \mathbf{p}^2$ in the numerator. The first term in the integral gives then just the integral $I_0(p)$ in Eq. (35). Going through the same steps as above with insertion of complete sets of states, the second term is then reduced to the finite integral $B_0(p)$. In this way we obtain

$$B'_2(p) = M I_0(p) + [p^2 - \alpha M \mu] B_0(p) \quad (\text{A5})$$

which again is a surprising simple result.

We notice that these three divergent Coulomb integrals contain the common factor $p^2 - \alpha M \mu$ in the results. This can be understood as coming from the divergence of the double derivative of the Coulomb wave function $\psi_{\mathbf{p}}(\mathbf{r})$ at the origin. It satisfies the Schödinger wave equation

$$\left[-\frac{1}{M} \nabla^2 + V_C(r) \right] \psi_{\mathbf{p}}(\mathbf{r}) = E \psi_{\mathbf{p}}(\mathbf{r}),$$

where the energy $E = p^2/M$. When we now take the limit $r \rightarrow 0$, it follows that

$$-\nabla^2 \psi_{\mathbf{p}}(\mathbf{r})_{r \rightarrow 0} = [p^2 - \alpha M \mu] \psi_{\mathbf{p}}(0) \quad (\text{A6})$$

since the regularized integral (A2) is just the Coulomb potential at the origin.

-
- [1] J.N. Bahcall, Phys. Rev. D **58**, 096016 (1998); *Neutrino Astrophysics* (Cambridge University Press, Cambridge, 1989).
[2] H.A. Bethe and C.L. Critchfield, Phys. Rev. **54**, 248 (1938).
[3] E.E. Salpeter, Phys. Rev. **88**, 547 (1952).
[4] J.N. Bahcall and R.M. May, Astrophys. J. **155**, 501 (1969).
[5] M. Kamionkowski and J.N. Bahcall, Astrophys. J. **420**, 884 (1994).
[6] R. Schiavilla, V.G.J. Stoks, W. Glöckle, H. Kamada, A. Nogga, J. Carlson, R. Machleidt, V.R. Pandharipande, R.B. Wiringa, A. Kievsky, S. Rosati, and M. Viviani, Phys. Rev. C **58**, 1263 (1998).
[7] A.N. Ivanov, N.I. Troitskaya, M. Faber, and H. Oberhummer,

- Nucl. Phys. **A617**, 414 (1997); **A618**, 509(E) (1997); **A625**, 896 (1997); H. Oberhummer, A.N. Ivanov, N.I. Troitskaya, and M. Faber, astro-ph/9705119.
[8] J.N. Bahcall and M. Kamionkowski, Nucl. Phys. **A625**, 893 (1997).
[9] A.N. Ivanov, H. Oberhummer, N.I. Troitskaya, and M. Faber, nucl-th/9910021.
[10] T.-S. Park, K. Kubodera, D.-P. Min, and M. Rho, Astrophys. J. **507**, 443 (1998).
[11] D.B. Kaplan, M.J. Savage, and M.B. Wise, Phys. Lett. B **424**, 390 (1998); Nucl. Phys. **B534**, 329 (1998).

- [12] D.B. Kaplan, M.J. Savage, and M.B. Wise, *Phys. Rev. C* **59**, 617 (1999).
- [13] J. Gegelia, *Phys. Lett. B* **429**, 227 (1998).
- [14] U. van Kolck, hep-ph/9711222; *Nucl. Phys.* **A645**, 273 (1999).
- [15] *Nuclear Physics with Effective Field Theory II*, edited by P.F. Bedaque, M.J. Savage, R. Seki, and U. van Kolck (World Scientific, Singapore, 2000).
- [16] J.-W. Chen, G. Rupak, and M.J. Savage, *Nucl. Phys.* **A653**, 386 (1999).
- [17] X. Kong and F. Ravndal, *Phys. Lett. B* **450**, 320 (1999).
- [18] J.D. Jackson and J.M. Blatt, *Rev. Mod. Phys.* **22**, 77 (1950).
- [19] X. Kong and F. Ravndal, *Nucl. Phys.* **A665**, 137 (2000).
- [20] X. Kong and F. Ravndal, *Nucl. Phys.* **A656**, 421 (1999).
- [21] X. Kong and F. Ravndal, *Phys. Lett. B* **470**, 1 (1999).
- [22] M. Butler, J.-W. Chen, and X. Kong, nucl-th/0008032.
- [23] D.R. Phillips, G. Rupak, and M.J. Savage, *Phys. Lett. B* **473**, 209 (2000).
- [24] M.G. Bowler, *Nuclear Physics* (Pergamon, London, 1973).
- [25] A. Sommerfeld, *Atombau und Spektrallinien*, Vol. II (Vieweg, Braunschweig, 1939); L.D. Landau and E.M. Lifschitz, *Quantum Mechanics* (Pergamon, London, 1958).
- [26] T. Mehen and I.W. Stewart, *Phys. Lett. B* **445**, 378 (1999); *Phys. Rev. C* **59**, 2365 (1999).
- [27] H.A. Bethe, *Phys. Rev.* **76**, 38 (1949).
- [28] M. Abramowitz and I.A. Stegun, *Handbook of Mathematical Functions* (Dover, New York, 1972).
- [29] J.-W. Chen and M. Savage, *Phys. Rev. C* **60**, 065205 (1999).
- [30] G. Rupak, *Nucl. Phys.* **A678**, 405 (2000).
- [31] P.F. Bedaque, H.W. Hammer, and U. van Kolck, *Nucl. Phys.* **A676**, 357 (2000).
- [32] M. Butler and J.-W. Chen, nucl-th/0101017.